Particle-hole strength excited in the ^{40}Ca(p,n)^{40}Sc reaction at 134 MeV

T. Chittrakarn, B. D. Anderson, A. R. Baldwin, C. Lebo, R. Madey, and J. W. Watson
Department of Physics, Kent State University, Kent, Ohio 44242

C. C. Foster
Indiana University Cyclotron Facility, Bloomington, Indiana 47405
(Received 11 February 1986)

The ^{40}Ca(p,n)^{40}Sc reaction was studied at 134 MeV. Neutron energy spectra were measured by the time-of-flight technique with resolutions of 220 keV at angles from 0° to 41° and 415 keV out to 62°. The $2^-,3^-,4^-,5^-$ band of states based on the $(f_{7/2},d_{3/2}^{-1})$ 1p1h structure was observed at low excitation energies, in good agreement with known analog states in ^{40}Ca and ^{40}K. The shapes of the cross-section and analyzing-power angular distributions are in good agreement with distorted-wave impulse-approximation calculations using simple 1p1h (Tamm-Dancoff approximation) shell-model wave functions. A relatively strong transition to a state at $E_x=2.3$ MeV with $L=3$ is identified tentatively as a 4^- state with the predominant 1p1h structure $(1f_{7/2},2s_{1/2}^{-1})$. The excitation of the $(T=1)$ 6^- $(f_{7/2},d_{5/2}^{-1})$ stretched state is observed near $E_x=7$ MeV, fragmented over approximately 3 MeV. The normalization factor required to make a distorted-wave impulse-approximation calculation agree in magnitude with the 6^- excitation is 0.35, which is larger than the normalization factor for this excitation in mass 28, analyzed in a similar manner. The $L=1$ giant resonance is observed to be centered near $E_x=10$ MeV with a width (full width at half maximum) of about 5 MeV, and a distorted-wave impulse-approximation normalization factor of 0.16. Two 1^+ excitations are observed at $E_x=2.7$ and 4.3 MeV which indicate directly the presence of ground-state correlations in the ^{40}Ca target. The fact that the analog of the higher 1^+ excitation is not seen in inelastic electron scattering indicates strong interference between spin and orbital current contributions. The effect of ground-state correlations on the 1p1h wave functions was investigated by performing calculations which allowed multiparticle-multihole correlations in the $d_{3/2}$ and $f_{7/2}$ orbitals. The distorted-wave impulse-approximation normalization factors obtained with these wave functions were found to increase by a factor of about 2 relative to those obtained with ^{40}Ca assumed to be a closed core.

I. INTRODUCTION

In several earlier papers[1-5] it was demonstrated that the (p,n) reaction at 135 MeV provides a good measure of one-particle, one-hole (1p1h) strength in spherical nuclei. This result follows because the reaction is apparently impulsive and dominated by single-scattering processes. Simple distorted-wave-impulse-approximation (DWIA) calculations are in good agreement with strong transitions. Part of this success must be attributed to the fact that isovector transitions are much less sensitive to density-dependent effects than are isoscalar transitions;[6] furthermore, 135 MeV appears to be an almost ideal beam energy for spectroscopic studies with the (p,n) reaction. This energy was chosen originally as a compromise between a higher energy where the reaction might be expected to be more impulsive, and a lower energy where the experimental resolution improves. Since now it appears that the (p,n) reaction becomes impulsive by about 100 MeV, this choice does not represent much of a compromise. [This result is observed to be true also for the (p,p') reaction.[7]] Another point in favor of 135 MeV is that more complicated optical potentials (such as so-called "wine-bottle" shapes[8]) may be required at higher (>200 MeV) energies which introduce further uncertainties into the theoretical description. The requirement for these shapes was observed to decrease as the proton energy decreases towards 100 MeV.[9]

The target nucleus for these studies (viz., ^{40}Ca) is a self-conjugate "doubly-magic" nucleus. The (p,n) reaction on a self-conjugate target excites only $T=1$ strength and offers an advantage over the (p,p') reaction for studies of isovector strength, since the latter reaction excites $T=0$ background strength as well. In an earlier paper, Fazely *et al.*[1] presented the results of a similar study on another such nucleus, ^{16}O. In that study, the (p,n) experimental results were compared with DWIA predictions based on simple wave functions which assumed ^{16}O to be a closed core and considered only 1p1h states of $1\hbar\omega$ and $2\hbar\omega$ excitation in the final nucleus [the Tamm-Dancoff approximation[10] (TDA)]. It was found that all of the strongest excitations observed were in good agreement with the theoretical predictions, both in excitation energy and in relative strength. Normalization factors required for the DWIA calculations were typically 0.25–0.40. A subsequent reanalysis of these measurements by Gareev *et al.*[11] which included 2p2h configurations in both the target and residual nuclei obtained normalization factors approximately twice as large.

We present here an analysis of the ^{40}Ca(p,n)^{40}Sc reac-

tion at 135 MeV which is similar to our earlier analysis of the $^{16}O(p,n)^{16}F$ reaction at 135 MeV. We present excitation-energy spectra at several angles out to 62° and angular distributions for the most strongly-excited states. The angular distributions are compared with DWIA calculations based on the TDA wave functions of Donnelly and Walker.[12] Similar also to the $^{16}O(p,n)^{16}F$ reaction, we see excitation of some 1^+ strength, which is a direct indication of ground-state correlations in the ^{40}Ca nucleus. The states excited are compared also with known analog-state excitations observed in (p,p') and (e,e') studies. Finally, we consider the effects of using a larger basis shell-model calculation for the low-lying states. These calculations, which include 2p2h and 4p4h correlations for the ^{40}Ca ground state, yield about a twofold increase in the DWIA normalization factors. These analyses reaffirm the idea that the (p,n) reaction at 135 MeV is basically impulsive and provides a good spectroscopic tool for identifying 1p1h strength in even-even nuclei.

II. EXPERIMENTAL PROCEDURE

The measurements were performed in two separate experimental runs; one with an unpolarized proton beam which provided cross-section measurements only, and one with a polarized proton beam to obtain analyzing-power measurements as well. For both runs, neutron time-of-flight spectra were obtained from the $^{40}Ca(p,n)^{40}Sc$ reaction with the beam-swinger system[13] at the Indiana University Cyclotron Facility (IUCF). Neutrons were detected in large-volume, mean-timed neutron detectors,[14] with overall time dispersions of 0.5—0.7 ns. Neutron time of flight was measured relative to the time of arrival of the beam on the target. This time was derived from a point of fixed phase of the cyclotron rf signal. A phase-compensation circuit[15] was used to eliminate drift between the time of arrival of a beam burst at the target and the cyclotron rf signal. A fast plastic scintillator monitored protons scattered elastically from the target to provide the necessary timing information to the phase-compensation circuit.

For the 135 MeV unpolarized proton-beam measurements, neutron detectors were placed in three separate detector stations at 0°, 24°, and 45° with respect to the undeflected proton beam, at distances of 125.2, 133.6, and 80.9 m, respectively, from the target. All the detectors were NE-102 fast-plastic scintillators 0.102 m thick. The 0° station contained three 0.508 m high by 1.02 m long neutron detectors which were combined to yield a total frontal area of 1.55 m^2. One 0.508 m high detector plus one 1.02 m high detector, both 1.02 m long, were used in the 24° station, also yielding a total frontal area of 1.55 m^2. Two 0.762 m high by 1.52 m long neutron detectors in the 45° station provided a total front area of 2.32 m^2. Charged-particle anticoincidence counters (0.953 or 1.27 cm thick) were placed in front and on top of each detector to veto charged particles from the target and cosmic rays.

For the 133.5 MeV polarized proton-beam measurements, neutron detectors were placed in three separate detector stations at 0°, 24°, and 45° with respect to the undeflected proton beam, at distances of 71.0, 71.0, and 37.3 m, respectively, from the target. Two 0.508 m high detectors, 1.02 m long, were used at 0°. One 0.508 m high detector plus one 1.02 m high detector, both 1.02 m long, were used at 24°. Two 0.762 m high by 1.52 m long neutron detectors were used in the 45° station. All the neutron detectors were 0.102 m thick. Similar to the unpolarized beam measurements, thin (0.95—1.27 cm thick) plastic scintillator detectors were placed in front and on top of the neutron detectors to veto charged particles from the target and cosmic rays.

Since the beam swinger is capable of deflecting the incident proton beam by 24°, neutron scattering angles from 0° to 24°, 24° to 48°, and 45° to 69° could be observed in the first, second, and third stations, respectively. The targets were made from calcium enriched to 99.97% ^{40}Ca. Thicknesses were determined with a "ball" micrometer and checked by weighing. The 133.5 MeV polarized-beam run used a target of thickness 29.2 mg/cm^2 to obtain the data for every angle. For the 135 MeV unpolarized-beam run, a 29.2 mg/cm^2 target was used at neutron scattering angles of 4°, 28°, and 49°, and a thinner target of 19.0 mg/cm^2 was used (to obtain better energy resolution) for the rest of the angles. The overall timing resolutions of 0.5—0.7 ns included contributions from the beam-burst width, the target thickness, the finite thickness of the neutron detectors, and the intrinsic timing resolutions of the detectors. For the polarized-beam run overall energy resolutions were about 250 keV out to 41° and about 415 keV at wider angles. For the unpolarized-beam run, the overall energy resolution with the thin (19.0 mg/cm^2) target was about 190 keV at 11.6° and about 220 keV at wider angles; the energy resolution with the thick (29.2 mg/cm^2) target was about 220 keV from 4° out to 28° and about 350 keV at wider angles.

The measured intensity of the neutron flux arriving at a detector was corrected for neutron scattering in the exit foil of the scattering chamber, the air, the wall of the detector station, and the anticoincidence detectors between the target and the detectors. The proton beam intensity was measured with a split Faraday cup, which was well shielded and located approximately 10 m downstream from the target. The beam integration was estimated to be accurate to about 5%. The measured flight paths are estimated to be known to within ±2 m, which corresponds to a maximum uncertainty of ±0.5% in the known solid angle (for the shortest flight path). In order to be able to calculate reliably the neutron detection efficiency, the pulse-height response of each counter was calibrated with a ^{232}Th radioactive gamma-ray source ($E_\gamma = 2.61$ MeV) and a fast amplifier. Neutron detection efficiencies were calculated with the improved Monte Carlo efficiency code of Cecil *et al.*[16] and tested by comparing various (p,n) and (p,p') analog transitions.[17,18] The neutron detection efficiencies determined in this way were checked previously[18] to be accurate to about ±10%. The overall scale uncertainty, which combines the above listed individual contributions, is estimated to be ±12%. The basic experimental procedure was described in more detail previously.[1]

III. DATA REDUCTION

The neutron time-of-flight (TOF) and detector pulse-height parameters were recorded event by event for each neutron detector. For the polarized-beam experiment, the spin state of the beam was recorded also. The event tapes were later replayed at several pulse-height thresholds in order to extract time-of-flight spectra, excitation-energy spectra, cross sections, and analyzing powers.

Excitation-energy spectra were obtained from the measured time-of-flight spectra by using the measured flight paths and the calibration of the time-to-amplitude converter. Known excitation energies of states in ^{40}Sc were taken to provide the absolute calibration of neutron energies. At forward angles, the strongly-excited 2^- state, assumed to be at $E_x=0.77$ MeV, was taken to provide this calibration; and at wide angles, the 5^- state, assumed to be at $E_x=0.89$ MeV was used. These excitation energies are taken from the compilation of Endt and van der Leun,[19] with the ordering of the 2^- and 5^- states assumed to be the same as observed for the analog states in ^{40}Ca and ^{40}K. These excitation energies were checked against the known 4^- ground-state excitation at wide angles. Extracted excitation energies are estimated to be accurate to ± 0.1 MeV.

Excitation-energy spectra at several angles are presented in Fig. 1. For the (p,n) spectra, there are three dominant sources of background: (1) cosmic rays, (2) overlap of slower neutrons from the previous beam burst, and (3) quasifree scattered (QFS) neutrons from (p,pn) reactions. After choosing a (software) pulse-height threshold which reduced overlap, while maintaining a reasonable detection efficiency, different runs at the same scattering angle were combined. Cosmic-ray backgrounds were determined from blank-target runs, and were subtracted channel by channel from the (p,n) spectra. The overlap of slow neutrons from the previous beam burst was observed as a small background in the TOF spectra at neutron energies corresponding to excitation energies below the ^{40}Sc ground state. Based on earlier studies performed with short flight paths in order to observe more of the continuum,[20,21] we assumed the "true" continuum was uniform in energy (to first order) and that the yield of such neutrons would simply reflect the detector efficiency as a function of energy. Thus, a slowly decreasing overlap spectrum was normalized to the background observed below the ground state for each spectrum, and subtracted channel by channel. The (p,n) spectra shown in Fig. 1 were corrected for cosmic-ray and overlap backgrounds in this manner.

Yields for individual transitions were extracted separately for spin-down, spin-up, and total spectra, by the techniques of simple peak summing and/or Gaussian peak fitting. Each spectrum was fitted in two regions with the improved peak-fitting code of Bevington.[22] The complexes of states from $E_x=0$–5.5 MeV were fitted simultaneously with Gaussian peaks which were required to have equal widths. [Note that the width could vary from one detector station to another (primarily because of the different flight paths) and for different runs.] Because the unbound characteristic of states in ^{40}Sc might be more significant at higher excitation energies (states become unbound in ^{40}Sc at $E_x=0.5$ MeV), the $L=1$ giant resonance region [from $5.5\leq E_x(\text{MeV})\leq 12$] was fitted by allowing the widths to vary. The error bars shown in the angular distributions were obtained from the error matrix of the fitting code; thus they are primarily statistical, but include a correction factor for the goodness of the fit (see Ref. 22 for more detail). A sample of the peak fitting results is shown in Fig. 2.

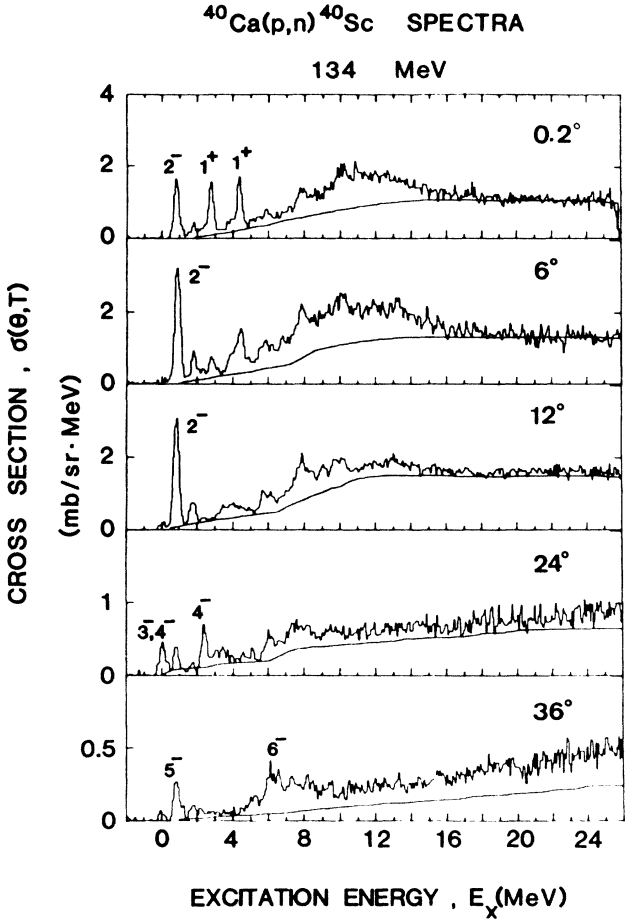

FIG. 1. Excitation-energy spectra for the ^{40}Ca(p,n)^{40}Sc reaction at 134 MeV after subtraction of cosmic-ray and overlap backgrounds. The solid lines represent a single-step quasifree scattering (QFS) calculation as described in the text.

The yields (Y) of individual transitions from summing and/or Gaussian peak fitting were combined with the known target thickness (t), detector solid-angle ($\Delta\Omega$), the calculated detector efficiencies (ϵ), the measured beam integration (I), the fractional livetime of the data-acquisition system (l), and the neutron transmission from the target to the detector (T) to obtain the differential cross section from the usual expression,

$$\sigma(\theta)=\frac{Y}{(It\Delta\Omega lT\epsilon)} . \tag{1}$$

For this experiment, all the detectors were on the right-hand side of the beam in the laboratory frame of reference; hence, by the Madison convention,[23] the analyzing power $A_y(\theta)$ is

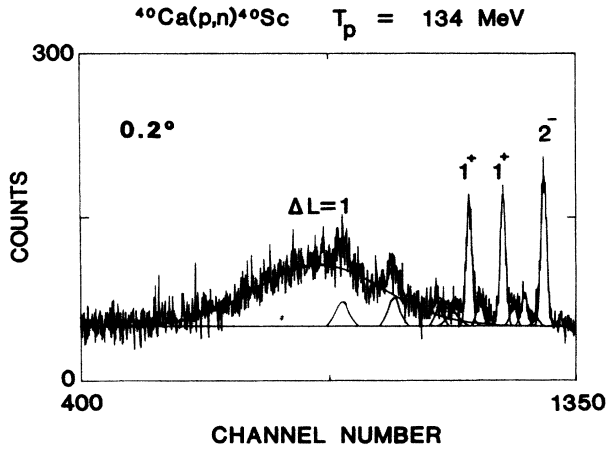

FIG. 2. An example of the peak-fitting results for the spectrum at 0.2°. Shown are fits to both narrow, low-lying states and to the broad $\Delta L = 1$ giant resonance.

$$A_y(\theta)=\frac{Y_\uparrow(\theta)-Y_\downarrow(\theta)}{P_\uparrow Y_\downarrow(\theta)+P_\downarrow Y_\uparrow(\theta)}\ , \tag{2}$$

where $Y_\downarrow(\theta)$ and $Y_\uparrow(\theta)$ are the yields in a single detector for the spin-down and spin-up states of the proton beam, and $P_\downarrow$ and $P_\uparrow$ are the polarizations for the spin-down and spin-up states of the proton beam. For $P_\downarrow = P_\uparrow = P_b$, the analyzing power $A_y(\theta)$ in Eq. (2) will simplify to

$$A_y(\theta)=\frac{Y_\uparrow(\theta)-Y_\downarrow(\theta)}{Y_\downarrow(\theta)+Y_\uparrow(\theta)}\frac{1}{P_b}=\frac{\epsilon}{P_b}\ , \tag{3}$$

where the asymmetry ϵ is

$$\epsilon=\frac{Y_\uparrow(\theta)-Y_\downarrow(\theta)}{Y_\downarrow(\theta)+Y_\uparrow(\theta)}\ . \tag{4}$$

The spin state of the beam was "flipped" every 60 s to reduce time-dependent asymmetries. The beam polarization was typically about 70%, as determined with a ^{4}He polarimeter located between the injector and main cyclotrons.[24]

IV. RESULTS

In order to identify specific transitions in this reaction, we subtracted a calculated quasifree scattering background from the spectra at each angle, extracted angular distributions for the observed states and complexes, and fitted the angular distributions with DWIA calculations based on known analog states and a TDA shell-model calculation to suggest initial choices for possible J^π values. This procedure and the results obtained are described below.

A. Quasifree background subtractions

The spectra presented in Fig. 1 show large excitation of the nuclear continuum. Recall that these spectra already have experimental backgrounds subtracted (viz., from cosmic rays and overlap from earlier beam bursts), so that the observed continua are "true" nuclear excitations. In earlier work, Anderson *et al.*[20] and Kalend *et al.*[21] concluded that the high-energy part of the continuum in forward-angle (p,n) spectra is dominated by single-step quasifree scattering [i.e., the (p,pn) reaction]. In another paper, Anderson *et al.*[4] showed that the continua in the ^{40}Ca(p,n)x and ^{48}Ca(p,n)x reactions could be described by a simple plane-wave impulse-approximation (PWIA) calculation with the *same* normalization factor for both reactions at each angle.

The QFS calculations adopted here are improved from those presented in Refs. 20 and 21 to include at least a partial accounting for Pauli-blocking effects. Basically, a kinematic condition is impressed to require that the difference between the sum of the final momentum of the observed neutron and the recoil momentum of the nucleus must be greater (in absolute magnitude) than the Fermi momentum of nucleons inside the nucleus. Actually, the Fermi momentum assumed for the nucleus in the nucleons is varied to obtain the best agreement between the calculations and the measured continuum spectra. This technique is, of course, a simplified accounting for a complex physical process; however, we do find an improved agreement between the calculations and the continuum spectra when this kinematic condition is required. The results of these calculations for this reaction are shown plotted on the experimental spectra of Fig. 1. The normalizations were chosen to make the calculations pass through the continuum near $E_x = 25$ MeV for angles out to 18°. (The single-step QFS calculations have a broad maximum near this excitation energy and will begin to fall away from the observed continuum at higher excitation energies, where multistep processes become important. See Refs. 20 and 21 for further discussion of these shapes.) Beyond 18°, the shape of the measured continua begin to deviate from the shape of the calculated spectra as one proceeds towards higher excitation energies; specifically, the experimental spectra are seen to rise more steeply than the calculations. This difference is attributed to the neglect of multistep processes in the continuum calculations. Note that beyond 18° the strength of the continua decreases significantly with increasing angle, which is expected for the single-step process; however, as the single-step contribution falls off, the smaller multistep processes become relatively more important, thereby making the continuum rise faster with increasing excitation energy than indicated by the single-step QFS calculations. We adopted these QFS calculations as a first-order background subtraction for the nuclear continuum at forward angles. This subtraction facilitates an analysis of the observed peaks and resonances. At low excitation energies, this subtraction is negligible and introduces no additional uncertainty in extracted strengths. Especially for the $L = 1$ giant resonance and slightly for the 6^- strength, both observed above $E_x = 5$ MeV, the total strength extracted is sensitive to the total background extracted. This sensitivity is discussed further below.

B. Comparison with 1p1h structure calculations

The excitation-energy spectra obtained after subtracting the single-step QFS calculations are shown in Fig. 3.

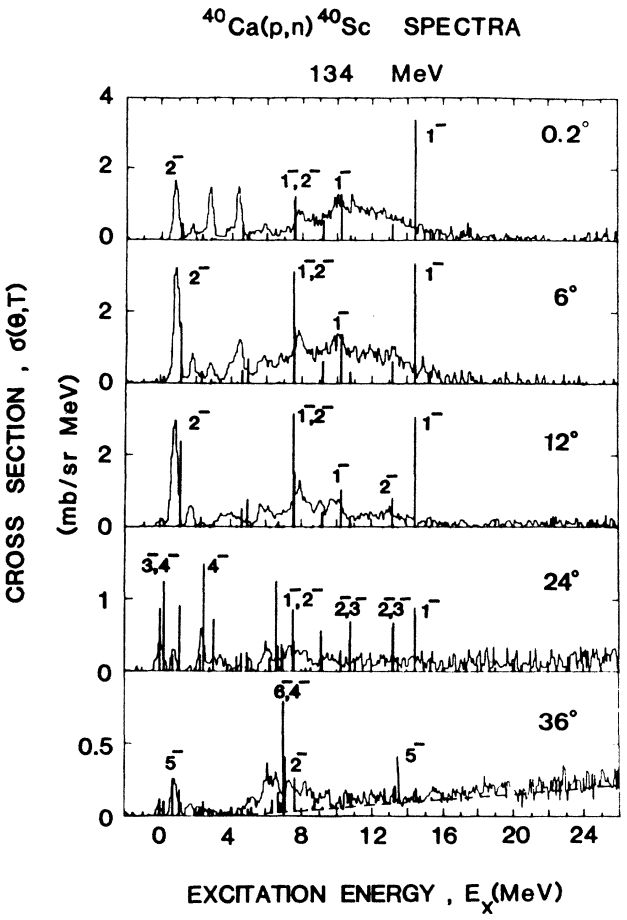

FIG. 3. Excitation-energy spectra after subtracting the calculated QFS backgrounds shown in Fig. 1. The vertical lines represent the results of DWIA calculations using the TDA shell-model wave functions of Ref. 12. The normalizations of the DWIA calculations are arbitrary, but are the same for all the calculations at each angle.

Shown also in these spectra are the results of DWIA calculations for the ^{40}Ca(p,n)^{40}Sc reaction with the 1p1h (TDA) wave functions of Donnelly and Walker (DW).[12] The DWIA calculations were performed with the code DW81,[25] with optical-model parameters from the global parameters of Schwandt *et al.*,[24] and the nucleon-nucleon effective interaction of Franey and Love.[26] The structure calculations are Tamm-Dancoff-approximation shell-model wave functions. The target nucleus ^{40}Ca is considered to be a closed core and particles are considered to be excited into the $1f$-$2p$ shell, leaving holes in the $1d$-$2s$ shell. Harmonic-oscillator eigenfunctions were assumed for the single-particle orbitals. The residual interaction was taken to be a Serber-Yukawa potential adjusted to fit low-energy n-p scattering. These calculations are similar to those performed also by Donnelly and Walker for $T=1$ states in ^{16}O and which we saw were in good agreement with the strongest transitions observed in the ^{16}O(p,n)^{16}F reaction at 135 MeV.[1]

The results of the DWIA calculations are shown in Fig. 3 with the same arbitrary normalization factor at each angle so that the relative strengths of the various excitations can be seen. The calculations of Donnelly and Walker are for $T=1$ states in ^{40}Ca. The lowest-energy state they predict is a 4^- state at $E_x=7.82$ MeV, which we take to be the energy corresponding to the known 4^- ground state of ^{40}Sc. The known energy of the $T=1$, 4^- state in ^{40}Ca is 7.66 MeV, which is within 200 keV of their calculation. Thus, the excitation energies shown for the calculations in Fig. 3 are the calculated energies reported by Donnelly and Walker minus 7.82 MeV. No further adjustment of their predicted excitation energies was performed.

Inspection of Fig. 3 shows that strong excitations are generally observed corresponding to the predicted strong excitations. In particular, two excitations are observed near $E_x=0$ and 1 MeV, which are predicted to correspond to a $3^-,4^-$ complex and a $2^-,5^-$ complex, respectively. A strong excitation is observed near $E_x=8$ MeV which agrees well with a predicted $1^-,2^-$ complex. In general, a large amount of 0^-, 1^-, and 2^- strength is predicted over the general region of the strong $L=1$ resonance observed between 7 and 18 MeV. A strong 4^- excitation is predicted near $E_x=2$ MeV, apparently in good agreement with a peak observed to be the largest in the spectrum at 24°. Finally, at wide angles a broadly distributed amount of strength is seen to be centered near the predicted location of a 6^- state. As will be discussed below, the observed angular distributions for these excitations are generally in good agreement with the predicted shapes from DWIA calculations for the states indicated.

The most noticeable disagreements between the predictions and the observed spectra are for the two peaks seen near $E_x=2.7$ and 4.3 MeV in the 0° spectrum. No strong excitations are indicated by the calculations at these energies for 0°. Some $L=1$ strength (0^-, 1^-, and 2^-) is predicted in this region, but clearly not in good agreement with that observed. As will be discussed further below, these two excitations involve strength based on ground-state correlations which are not included in the TDA calculations. The predicted excitation energies and amplitudes of the principal configurations for the states of interest in this work are listed in Table I.

C. Individual transitions

Let us now consider "individual" transitions. Actually, the excitations observed are almost always complexes of two or more peaks which are unresolved. Sometimes the states involved have very different angular distributions so that the individual contributions can be extracted.

1. The $3^-,4^-$ ground-state complex

The ground state of ^{40}Sc is known to have $J^\pi=4^-$. Another state is known at $E_x=0.03$ MeV, which could not be resolved in this experiment. The analogs of these two $T=1$ states are known[19] in both ^{40}Ca and ^{40}K. In both nuclei, the lower state is a 4^- state and the upper state is a 3^- state. The shell-model calculation of Donnelly and Walker predicts a 4^- ground state with a 3^- state about 200 keV higher. Both of these states are indicated by the shell-model calculations to have the predominant $(f_{7/2},d_{3/2}^{-1})$ 1p1h structure (see Table I).

TABLE I. Principal transitions and amplitudes assumed.

Excitation energy (MeV) Expt.	Theor.	J^π	Principal transition	Amplitude (OBTD)[c]	Ref.
0.00[a]	0.00	4^-	$1d_{3/2}\rightarrow 1f_{7/2}$	0.993	12
0.03[a]	0.23	3^-	$1d_{3/2}\rightarrow 1f_{7/2}$	0.979	12
0.77[a]	1.11	2^-	$1d_{3/2}\rightarrow 1f_{7/2}$	0.967	12
0.89[a]	0.73	5^-	$1d_{3/2}\rightarrow 1f_{7/2}$	0.997	12
2.3[b]	2.7	4^-	$2s_{1/2}\rightarrow 1f_{7/2}$	0.984	12
2.7[b]	3.1	1^+	$1d_{3/2}\rightarrow 1d_{3/2}$	−0.224	31,32
			$1f_{7/2}\rightarrow 1f_{7/2}$	0.039	
	4.1	1^+	$1d_{3/2}\rightarrow 1d_{3/2}$	−0.091	31,32
			$1f_{7/2}\rightarrow 1f_{7/2}$	−0.134	
4.3[b]	4.4	1^+	$1d_{3/2}\rightarrow 1d_{3/2}$	0.078	31,32
			$1f_{7/2}\rightarrow 1f_{7/2}$	0.086	
	4.8	1^+	$1d_{3/2}\rightarrow 1d_{3/2}$	0.001	31,32
			$1f_{7/2}\rightarrow 1f_{7/2}$	−0.077	
5–10[b]	6.9	6^-	$1d_{5/2}\rightarrow 1f_{7/2}$	1.000	12
6–18[b]	6–16	$0^-,1^-,2^-$	$1d2s\rightarrow 1f2p$		12

[a]From Endt and van der Leun, Ref. 19.
[b]From this work.
[c]One-body transition densities.

The experimental angular distribution for this complex is shown in Fig. 4. The angular distribution is seen to peak near 20°. The transition to either a 3^- or a 4^- state would be predominantly $L=3$ (the latter with $\Delta S=1$). The DWIA calculations for these two transitions are also shown in Fig. 4; in fact, one sees that the two angular distributions are similar in shape, which makes it impossible to determine the relative contributions. The experimental shape is described well by the sum of the two calculations with a normalization factor for each state of 0.09, which seems to be a rather small normalization factor, especially compared to some of the other transitions discussed below.

Because the experimental angular distribution shows no evidence for a state with a predominant L transfer different than $L=3$, we assume that these two low-lying states are the analogs of the 3^- and 4^- $T=1$ states known in ^{40}Ca and ^{40}K. The 4^- state is known to be the ground state of ^{40}Sc. It must be emphasized that these measurements, by themselves, present no evidence for more than one state; however, two are known[19] to be within 30 keV of each other and would not be resolved here.

The products of the measured cross sections and analyzing powers for this complex are shown in Fig. 5 compared to the DWIA sum for the two transitions to a 3^- and a 4^- state. The same normalization factor ($N=0.09$) is used here as for the cross section comparisons of Fig. 4. The agreement between the measurements and the calculations is quite good, providing no evidence that the dominant strength excited does not have the assumed structures or that the DWIA calculations are not reasonable. Of course, the small spectroscopic factor required for this complex is bothersome, and we will discuss this further below.

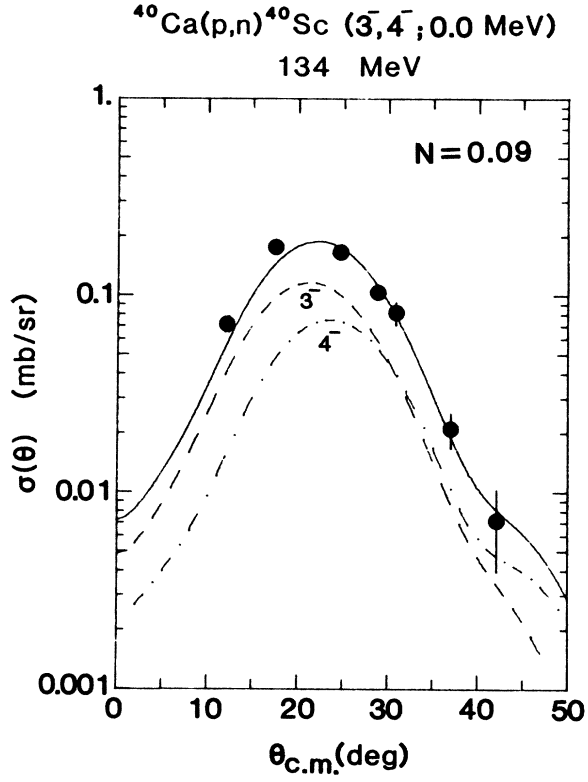

FIG. 4. Cross-section angular distribution for the ^{40}Ca(p,n)^{40}Sc reaction at 134 MeV to the 3^-,4^- ground-state complex. The dashed and dashed-dotted curves represent DWIA calculations for the 3^- and 4^- transitions individually, and the solid curve for their sum. The calculations use the TDA wave functions of Ref. 12 (see text).

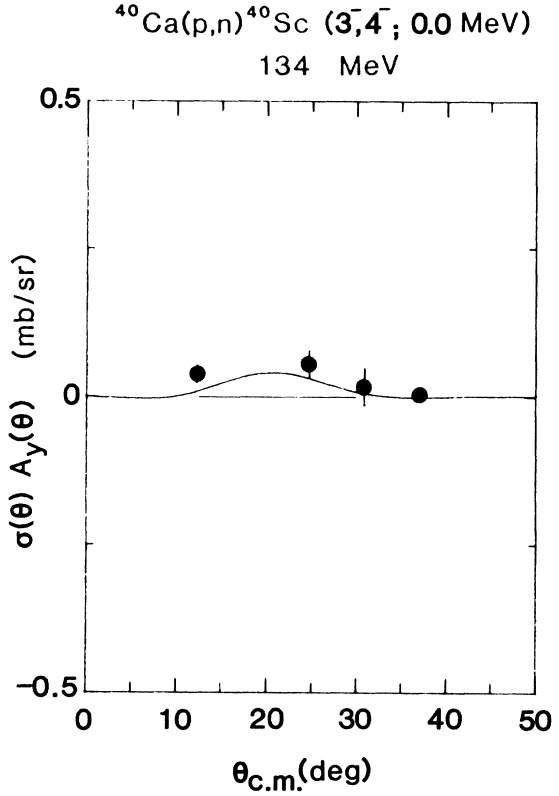

FIG. 5. Angular distribution for the product of the cross section and the analyzing power for the 3^-,4^- ground-state complex transitions. The solid curve represents the sum of DWIA calculations for this product for the 3^- and 4^- transitions performed separately. (See Fig. 1 and text for more details.)

2. The 2^-,5^- complex at 0.85 MeV

The second and third excited states of ^{40}Sc are known to be at $E_x=0.77$ and 0.89 MeV, respectively. These two states are likely to be the analogs of known 2^- and 5^- states observed about 0.9 MeV above the $T=1$, 4^- states in ^{40}Ca and ^{40}K. The measured cross-section angular distribution for this complex is shown in Fig. 6. A primary peak is observed near 10° and a secondary maximum near 35°. DWIA calculations for a 2^- and a 5^- state are shown, similar to those described above for the ground-state complex. The TDA structure wave functions are again predominantly $(f_{7/2},d_{3/2}^{-1})$ for these two states.[12] (See Table I.)

The sum of the two calculations is seen to describe the data well with a normalization factor N of 0.18 for the 2^- transition and 0.20 for the 5^- transition. These calculations indicate that the first maximum is due primarily to the 2^- transition and that the second maximum is due predominantly to the 5^- transition, but that the latter includes a significant amount of strength from a secondary maximum in the calculated 2^- angular distribution.

This experiment shows no indication of the existence of a third state in this complex. Although the energy resolution of this experiment does not enable us to determine the ordering of the 2^- and 5^- states in this nucleus, probably the 2^- state is the lower one (at 0.77 MeV) and the 5^- state the higher one (at 0.85 MeV) since this is the ordering observed for the analogs of these two states in both ^{40}Ca and ^{40}K.

The products of the measured cross sections and analyzing powers for this complex are shown in Fig. 7 compared to the DWIA calculated sum for the 2^- and 5^- transitions. The same normalization factors are used here as for the cross section comparisons of Fig. 6. The shape of the experimental angular distribution is seen to be quite different from that for the ground-state complex and again to be reproduced quite well by the DWIA calculations.

3. The 1^+ state at 2.7 MeV

The 0° spectrum (see Figs. 1 and 3) shows three relatively strong excitations at low excitation energies. The lowest one is observed at $E_x=0.9$ MeV and is the 2^-,5^- complex discussed above. The next peak is observed at $E_x=2.7$ MeV. The experimental cross section angular distribution for this peak is shown in Fig. 8 and is seen to be peaked strongly at 0°. This peak must be the excitation

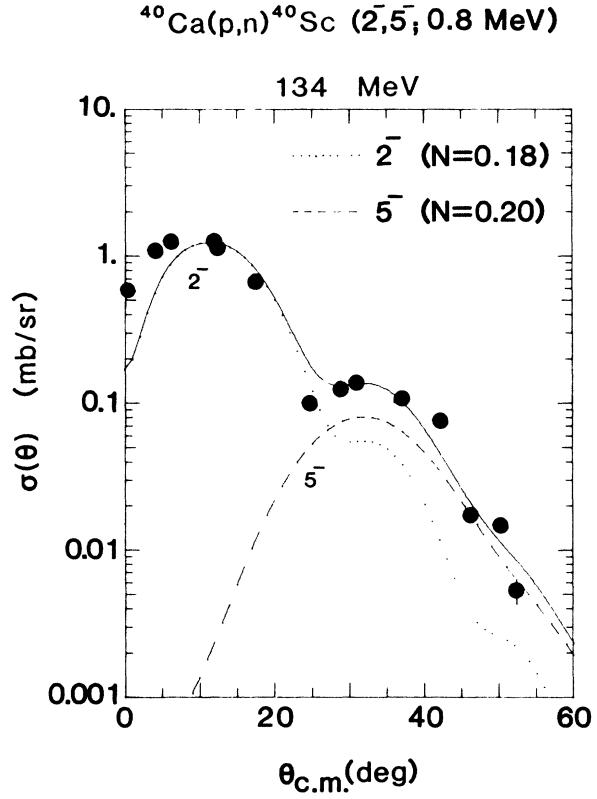

FIG. 6. Cross-section angular distribution for the ^{40}Ca(p,n)^{40}Sc reaction at 134 MeV to the 2^-,5^- complex at 0.85 MeV. The dotted and dashed curves represent DWIA calculations for the 2^- and 5^- transitions individually, and the solid curve for their sum. The calculations use the TDA wave functions of Ref. 12 (see text).

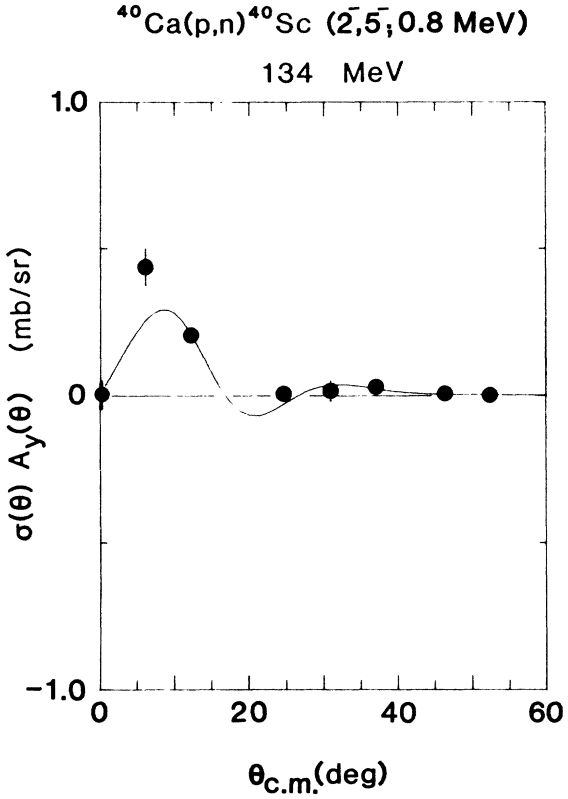

FIG. 7. Angular distribution for the product of cross section times analyzing power for the $2^-,5^-$ complex at 0.85 MeV. The solid curve represents the sum of DWIA calculations for the 2^- and 5^- transitions performed separately. (See Fig. 6 and text for more details.)

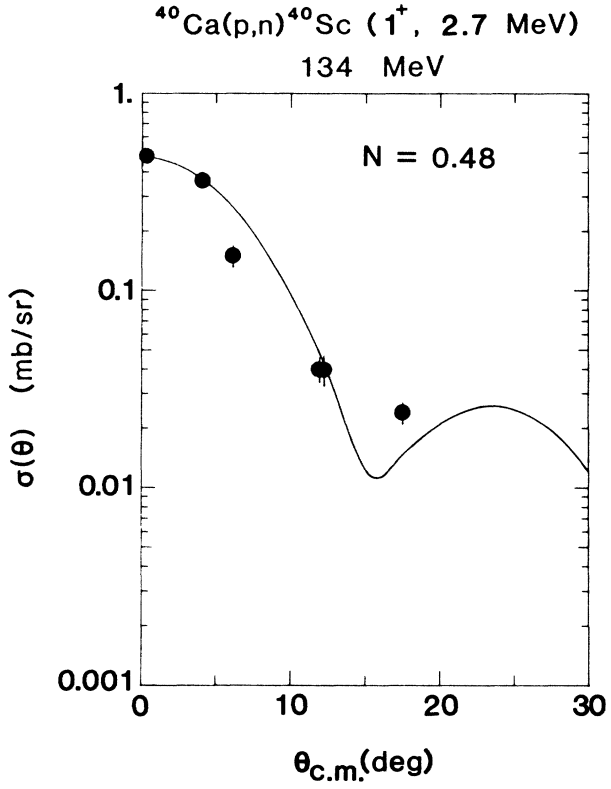

FIG. 8. Cross section angular distribution for the ^{40}Ca(p,n)^{40}Sc reaction at 134 MeV to the 1^+ state at 2.7 MeV. The solid curve represents a DWIA calculation with shell-model wave functions based on multiparticle-multihole correlations in the ^{40}Ca target nucleus (see text).

of the analog of a 1^+ state observed in ^{40}Ca via inelastic electron [27] and proton[28] scattering at $E_x = 10.3$ MeV. Recall that the analog of the 4^- ground state of ^{40}Sc is known to be at $E_x = 7.7$ MeV in ^{40}Ca; hence $E_x = 2.7$ MeV in ^{40}Sc corresponds to $E_x = 10.4$ MeV in ^{40}Ca. This 1^+ excitation in ^{40}Sc was also observed in the (p,n) studies of Taddeucci *et al.*[29]

Since a low-lying positive-parity excitation can arise only from ground-state correlations in the ^{40}Ca target nucleus, the existence of this excitation indicates directly the presence of such correlations. Note that the strength of this transition is relatively weak for a "Gamow-Teller" transition in the (p,n) reaction; for example, the low-lying 1^+ excitation (at $E_x = 2.52$ MeV) observed in the ^{48}Ca(p,n)^{48}Sc reaction at 134 MeV is more than 15 times stronger.[4] If one assumes that the 1^+ state in ^{48}Sc has a predominant structure of $(f_{7/2}, f_{7/2}^{-1})$, and that the transition is from the eight excess neutrons in ^{48}Ca, then the observed 1^+ cross section in the ^{40}Ca(p,n)^{40}Sc reaction corresponds to approximately one-half of a neutron (or actually one-half of a proton hole). This result is consistent with measured pickup spectroscopic factors for the $d_{3/2}$ orbital in ^{40}Ca.[30]

Shown also in Fig. 8 is a DWIA calculation similar to those described above, but with wave functions for both the ^{40}Ca target and the ^{40}Sc residual nucleus which include multiparticle-multihole configurations. The shell-model code OXBASH of Brown *et al.*[31] with the interaction of Sakakura, Arima, and Sebe[32] was used to perform the shell-model calculations. The basis allowed consists of only the $1d_{3/2}$ and $1f_{7/2}$ orbitals. These calculations yield many 1^+ states for ^{40}Sc, but only the lowest four have significant strength in the (p,n) reaction. Of these four 1^+ states, the lowest one is calculated to have the largest (p,n) cross section and is predicted to be at $E_x = 3.1$ MeV, within 0.4 MeV of the observed 1^+ state at 2.7 MeV (see Table I). The DWIA prediction for this state is shown in Figs. 8 and 9. The calculated cross section angular distribution is seen to agree well with the data and the calculated analyzing powers are in reasonable agreement, especially considering the relatively large error bars on the analyzing-power data. The normalization factor required to make the DWIA calculations agree in magnitude with the experimental cross sections is 0.48. This normalization factor is similar to that required for the comparison of DWIA calculations for the 1^+ excitations in the ^{48}Ca(p,n)^{48}Sc reaction;[4] however, in the latter case, the 1^+ excitations come primarily from transitions allowed in the simple shell model, while in the present case this 1^+ transition must be due to core correlations,

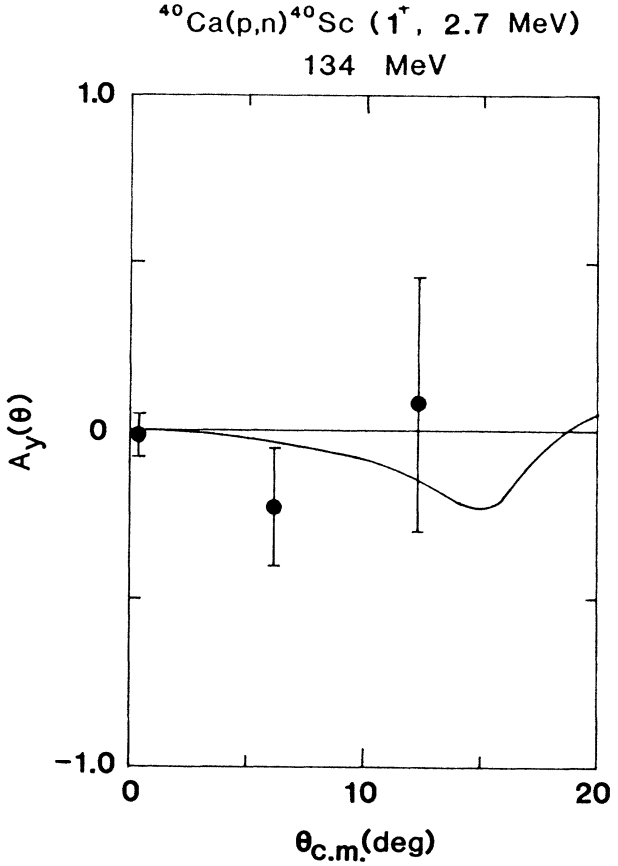

FIG. 9. Analyzing-power distribution for the transition to the 1^+ state at 2.7 MeV. The solid curve represents a DWIA calculation. See Fig. 8 and text for more details.

and the DWIA calculation must use wave functions which try to estimate these correlations.

4. The 1^+ complex at 4 MeV

The third strong low-lying excitation observed in the 0° spectrum is at 4.3 MeV. This transition falls off dramatically away from 0°, where it merges into a complex extending down to about 3.9 MeV. At 12°, the lower part of this complex dominates, and at wider angles, the whole complex rapidly diminishes. This complex consists of at least two peaks: one at 4.3 MeV, which clearly dominates the complex at 0°, and the other at 3.9 MeV. The fact that there are at least two peaks is seen clearly in the 4° spectrum shown in Fig. 10. This spectrum was obtained in the unpolarized-beam experimental run with a flight path of 125.2 m and an overall energy resolution of 210 keV. (Unfortunately, no 0° run was performed in the unpolarized-beam experimental run.)

Because Fig. 10 shows this complex to consist of (at least) two peaks, we fit the complex at all angles (out to 12°) with two peaks; one at $E_x = 4.3$ MeV and one near $E_x = 3.9$ MeV. The angular distributions obtained for these two peaks are shown in Figs. 11 and 12. Note that the results for the 4° and 11.6° runs (with the longer 125 m flight path of the unpolarized-beam experimental run)

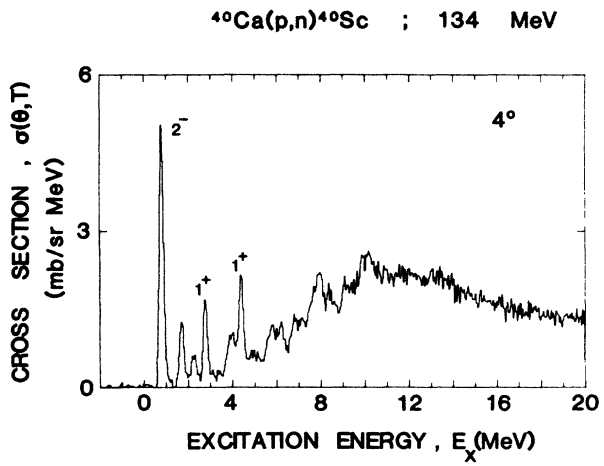

FIG. 10. Excitation-energy spectrum for the ^{40}Ca(p,n)^{40}Sc reaction at 134 MeV and 4°.

are consistent with those from the 0.2°, 6°, and 12° runs (with the shorter 71 m flight path of the polarized-beam runs).

The angular distribution for the 4.3 MeV state shown in Fig. 11 is peaked strongly at 0°, which indicates an $L = 0$ transition to either a 0^+ or a 1^+ state. Because of the dominance of the $V_{\sigma\tau}$ term over the V_τ term in the N-N

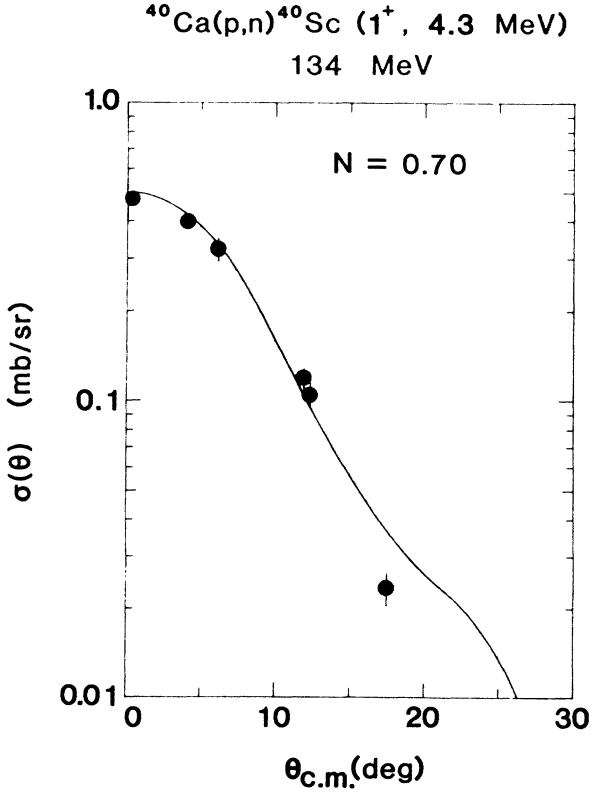

FIG. 11. Cross-section angular distribution for the ^{40}Ca(p,n)^{40}Sc reaction at 134 MeV to the 1^+ state at 4.3 MeV. The solid curve represents a DWIA calculation with shell-model wave functions based on multiparticle-multihole correlations in the ^{40}Ca target nucleus (see text).

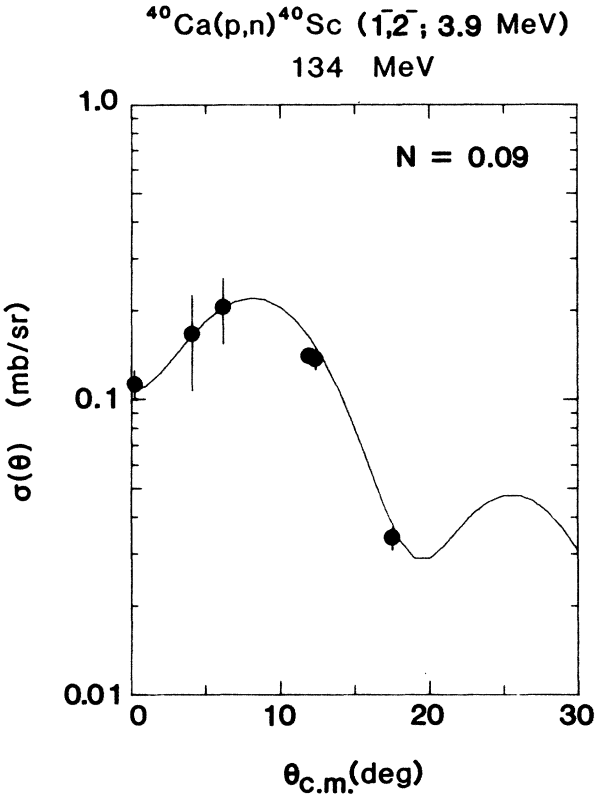

FIG. 12. Cross-section angular distribution for the ^{40}Ca(p,n)^{40}Sc reaction at 134 MeV to the $1^-,2^-$ complex at 3.9 MeV. The solid curve represents a DWIA calculation with the TDA wave functions of Ref. 12 (see text).

effective interaction at this energy, this state is almost certainly a 1^+ excitation. The excitation energy is in agreement with that observed for an $L=0$ transition in the ^{40}Ca(p,p') reaction at 200 MeV by Crawley *et al.*[28] They see strong $L=0$ transitions to states at 10.31 and 12.03 MeV in ^{40}Ca. If we take the known excitation energy (7.66 MeV) of the analog of the ground state of ^{40}Sc as the net displacement energy, these $L=0$ transitions would correspond to excitation energies in ^{40}Sc of 2.65 and 4.37 MeV, in good agreement with the $L=0$ transitions we see at 2.7 and 4.3 MeV. Also, Taddeucci *et al.*[29] note the strong excitation of the 4.3 MeV state at 0°, but because of poorer energy resolution, they were not able to extract an angular distribution for this transition.

As noted by Crawley *et al.*,[28] it is significant that the analog of the 4.3 MeV state is not seen in backward-angle inelastic electron scattering. This result indicates that this state has comparable spin and current contributions which largely cancel for the electron-scattering excitation. The (p,p') and (p,n) excitations, which are sensitive primarily only to the spin contribution, excite the state strongly. In an earlier paper, Anderson *et al.*[33] showed that such cancellations can, in general, be expected for certain excitations and are, in fact, observed in the $A=24$ system.

As discussed above, we performed a shell-model calculation for 1^+ excitations based on the $1d_{3/2}$ and $1f_{7/2}$ orbitals only, but allowing up to 4p4h excitations in the ^{40}Ca ground state. Only the four lowest 1^+ states were found to have significant (p,n) cross sections (with the DWIA). The lowest 1^+ state predicted was shown above compared to the observed transition to the state at 2.7 MeV. The next three states are predicted to be at 4.1, 4.4, and 4.8 MeV in ^{40}Sc (see Table I). These three states show similar angular distributions of both cross sections and analyzing powers. The predicted 0° cross sections are 0.37, 0.10, and 0.26 mb/sr, respectively. Since these three excitations are all quite similar, and located within ±0.5 MeV of the observed excitation at 4.3 MeV, we compare the combined cross sections for these three predicted states with the experimental angular distribution in Fig. 11. Correspondingly, we show the weighted average of the predicted analyzing powers for these three transitions in Fig. 13. The cross section angular distribution is seen to be described well with a normalization factor of 0.70. The predicted analyzing power angular distribution is seen to be similar to that predicted also for the lowest 1^+ state; however, the experimental analyzing powers are seen here to be positive near 10°, while the predicted analyzing powers are negative, and do not describe the data well.

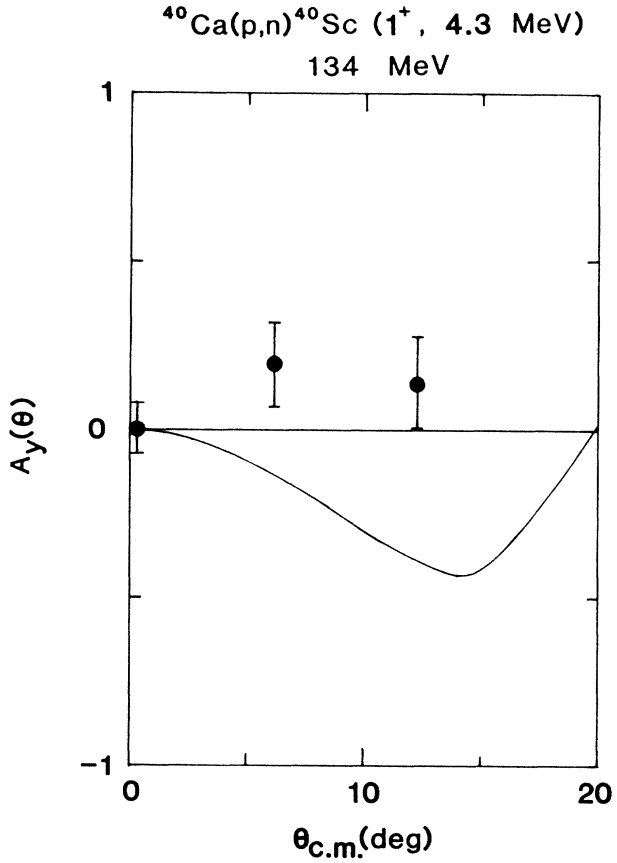

FIG. 13. Analyzing-power angular distribution for the transition to the 1^+ state at 4.3 MeV. The solid curve represents a DWIA calculation. See Fig. 11 and text for more details.

The angular distribution for the other half of the complex near $E_x = 4$ MeV, (i.e., for the 3.9 MeV peak) is shown in Fig. 12 and is fitted reasonably well by an $L = 1$ angular distribution. Because the TDA shell-model calculations predict relatively strong 1^- and 2^- states near this excitation energy (see Fig. 3), and because the (p,n) reaction excites primarily 1p1h strength, we tentatively assign this excitation as a $1^-,2^-$ complex.

5. *The 4^- complex at 2.3 MeV*

The last low-lying peak we wish to consider is a complex near 2.3 MeV which is seen to be the dominant low-lying transition at intermediate angles (as seen in the 24° spectrum of Fig. 3). The location of this excitation is in good agreement with a strong 4^- transition predicted by the DWIA calculations with the TDA wave functions. The angular distribution for this complex is shown in Fig. 14 compared with a DWIA calculation for four transitions predicted to be near this excitation energy. The agreement between the observed shape and the sum of the four transitions (to 0^-, 1^-, 3^-, and 4^- states) is seen to be reasonable. Note that the measured angular distribution for this complex indicates clearly a dominant $L = 3$ angular distribution beyond about 10°. Because the 4^- state is predicted to dominate this complex at wide angles, where the excitation energy is observed to be 2.3 MeV, we tentatively assign a 4^- state at that energy. The TDA shell-model calculations[12] indicate that the predominant 1p1h structure of this state is $(f_{7/2}, 2s_{1/2}^{-1})$.

6. *The $L = 1$ giant resonance between 6 and 18 MeV*

The largest total strength observed in this reaction is seen in a broad resonance between about 6 and 18 MeV at forward angles. An angular distribution for this resonance was obtained by fitting the spectra of Fig. 3 (i.e., after the QFS subtractions) between $E_x = 6$ and 18 MeV, for angles out to 30°; beyond 30°, as noted earlier, the simple QFS calculation no longer accounts for the observed continuum (because multistep processes are important) and a linear background shown, in Fig. 3, was, in addition, subtracted. The resulting angular distribution is shown in Fig. 15. The angular distribution is peaked near 10°, which indicates a strong $L = 1$ contribution.

Shown also in Fig. 15 are DWIA calculations for all transitions predicted by the TDA shell-model calculations to lie in this energy region, normalized so that the sum

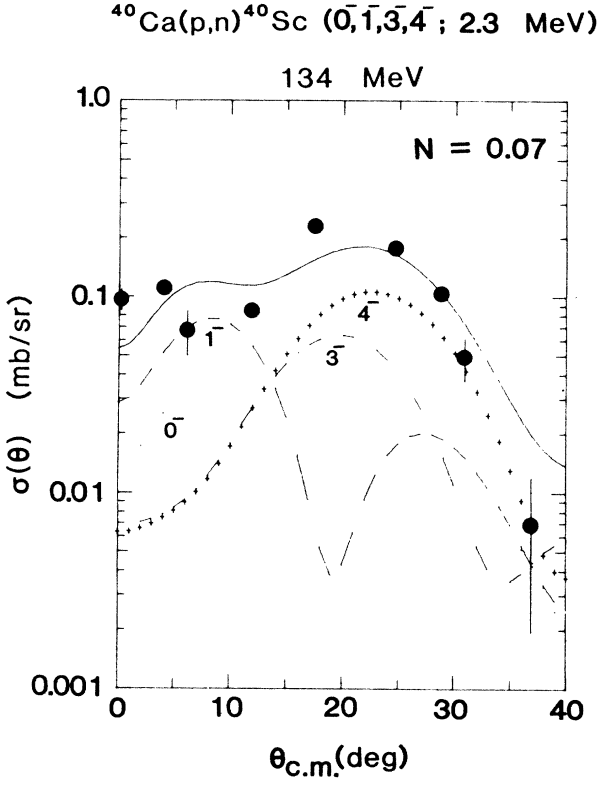

FIG. 14. Cross-section angular distribution for the $^{40}Ca(p,n)^{40}Sc$ reaction at 134 MeV to the $0^-,1^-,3^-,4^-$ complex at 2.3 Mev. The curves represent DWIA calculations with the TDA wave functions of Ref. 12 (see text).

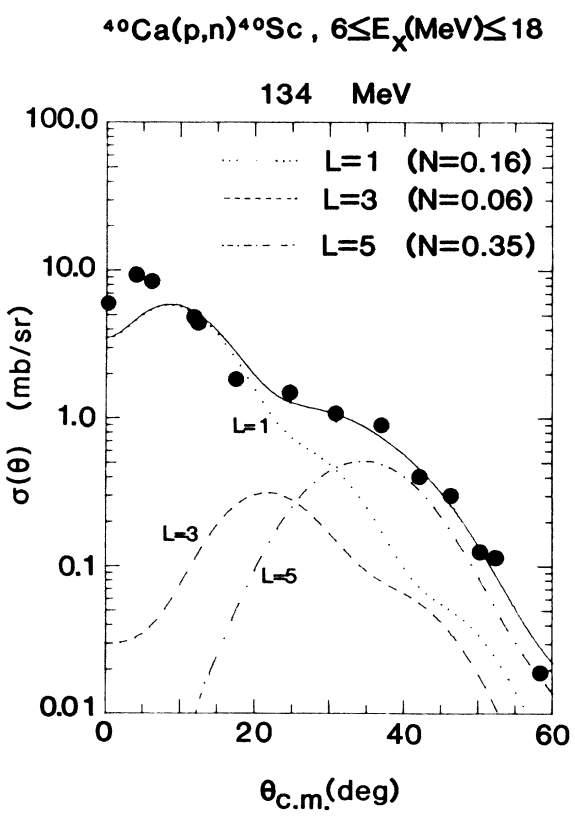

FIG. 15. Cross-section angular distribution for the $^{40}Ca(p,n)^{40}Sc$ reaction at 134 MeV to the complex of states between 6 and 18 MeV. The curves represent DWIA calculations with the TDA wave functions of Ref. 12 (see text).

provides the best overall fit to the data. The states predicted to lie in this region of excitation energy include 0^-, 1^-, 2^-, 3^-, 4^-, 5^-, and 6^- states. The 0^-, 1^-, and 2^- excitations proceed predominantly by $L=1$, the 3^- and 4^- excitations by $L=3$, and the 5^- and 6^- excitations by $L=5$. Because the predicted shapes for the different excitations with the same L transfer are similar, we cannot try to determine the relative normalizations for all seven transitions; accordingly, we have considered only the sum of all the transitions for each L transfer and then varied the relative normalizations for these three L transfers to try to fit the extracted angular distribution. The result is shown in Fig. 15. The sum of the transitions to the 0^-, 1^-, and 2^- states yield a normalization factor $N=0.16$. The contributions from transitions to 1^- and 2^- states are predicted to be much stronger than are those to 0^- states. The sum of the transitions to the 3^- and 4^- states requires $N=0.06$ and is never seen to be the most dominant L transfer. Finally, the sum of the 5^- and 6^- transitions requires $N=0.35$ and is seen to dominate the widest-angle part of the angular distribution. (This strength is analyzed further in the next section.) Note that although the sum of these three L transfers describes the experimental angular distribution fairly well beyond about 10°, it does not describe the data well near 0°. None of the calculated $L=1$ angular distributions (i.e., to a 0^-, 1^-, or 2^- state) is able to describe the data well at very forward angles. The easiest way to describe the region near 0° is to add some $L=0$ strength, which may be evidence for additional 1^+, Gamow-Teller strength in this energy region.

Returning to the $L=1$ strength, we see that because the angular distribution is peaked away from 0°, some $L=1$ strength is required. From our analysis, we have the result that the total $L=1$ spectroscopic strength observed is only 16% of that expected from the DWIA calculations using the TDA 1p1h wave functions. Thus, although the $L=1$ giant resonance dominates the forward-angle spectra, the total strength observed is only a small fraction of that expected assuming that the ^{40}Ca target nucleus is a simple closed core.

7. *The 6^- strength between 5 and 10 MeV*

In an earlier Letter[34] we reported the observation of fragmented $(f_{7/2}, d_{5/2}^{-1})$, 6^-, $T=1$ strength in the ^{40}Ca(p,n)^{40}Sc reaction. We present here a more detailed analysis of this excitation.

The wide-angle spectra of Figs. 1 and 3 show a complex of strength between 5 and 10 MeV of excitation. In Fig. 16 we show the angular distribution of the lower one-half of this strength (via., from $E_x=5$ to 7 MeV). This angular distribution is seen to be peaked near 40° and its shape is described well by a DWIA calculation for a transition

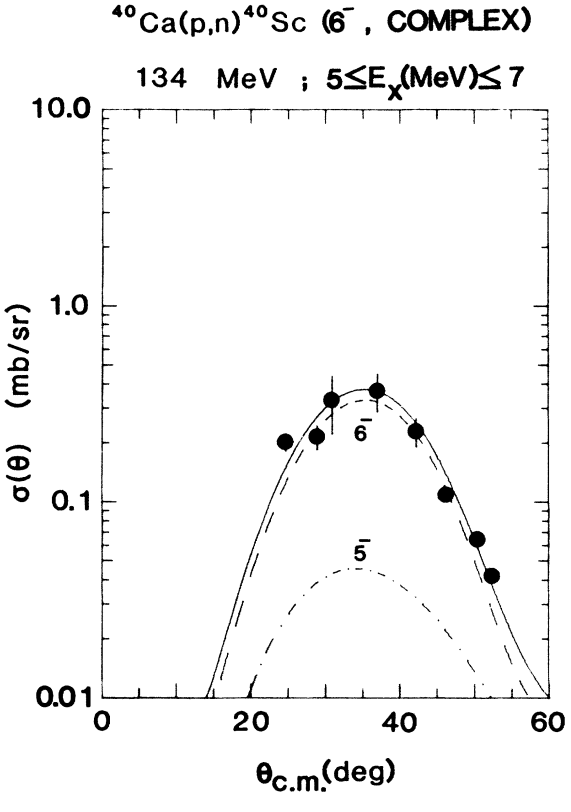

FIG. 16. Cross-section angular distribution for the ^{40}Ca(p,n)^{40}Sc reaction at 134 MeV to the part of the 6^- complex observed between 5 and 7 MeV. The curves represent DWIA calculations with the TDA wave functions of Ref. 12 (see text).

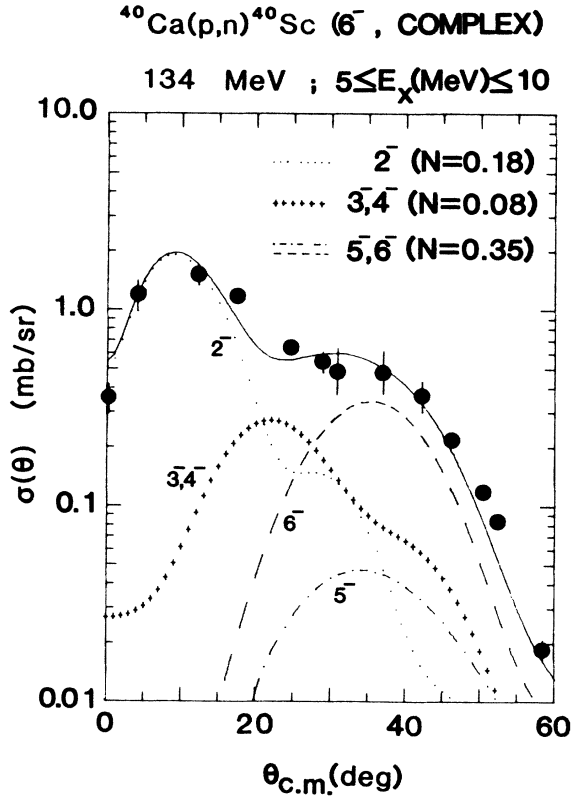

FIG. 17. Cross-section angular distribution for the ^{40}Ca(p,n)^{40}Sc reaction at 134 MeV to the full 6^- complex observed between 5 and 10 MeV. The curves represent DWIA calculations with the TDA wave functions of Ref. 12 (see text).

to a 6^- state. Thus we have good evidence for 6^- strength in this excitation-energy region. In Fig. 17 we show the angular distribution for the entire excitation-energy region out to 60°. The peak strength was extracted at wider angles by peak-fitting above the simple linear backgrounds similar to the one shown in Fig. 3.

The angular distribution for this entire complex is seen to be dominated by an $L=1$ transition at more forward angles (see the preceding subsection), to require some $L=3$ strength at intermediate angles, and to have a shoulder near 40° which requires $L=5$ strength, as shown. The normalization required for the total $L=5$ strength (i.e., the sum of the 5^- and 6^- strength) is 0.35. Note that the contribution of 5^- strength is predicted by the DWIA to be small compared to the 6^- contribution. This result occurs because transitions dominated by the tensor term of the N-N effective interaction will excite normal-parity transitions only via the exchange term, which is predicted to be weak.[26,35] This effect was confirmed experimentally in the observed relative excitations of the 6^+ and 7^+ states in the ^{48}Ca(p,n)^{48}Sc reaction reported earlier.[4] The 6^+ normal-parity transition was observed to be excited with less than 10% of the strength of the 7^+ non-normal parity transition; furthermore, the relative excitation of the 6^+ and 7^+ states was in good agreement with DWIA predictions for that reaction. Hence, we assume here that the DWIA can provide at least a good first-order estimate of the relative strengths of the 5^- and 6^- excitations.

Although the strength observed for the 6^- transition is assumed to be pure $(f_{7/2},d_{5/2}^{-1})$, it is observed to be highly fragmented. We ascribe this fragmentation primarily to the fragmentation of the $d_{5/2}$-hole state, which is far from the Fermi level in ^{40}Ca. As an orbital becomes further removed from the Fermi surface, the simple shell model no longer applies and the strength associated with a single shell-model orbital fragments. This fragmentation can be seen clearly for the $d_{5/2}$ orbital near $A=40$ in the ^{39}K(p,n)^{39}Ca spectrum shown in Fig. 18.[36] If the ground state of ^{39}K is a proton-hole state, then the (p,n) reaction will populate selectively the spectrum of neutron-hole states in ^{39}Ca. [In fact, we find that the (p,n) reaction at 0°, because the momenta transfer is small, is a powerful tool for mapping hole-state strength in odd-A nuclei.] From Fig. 18, we can see that while the $d_{3/2}$ orbital is concentrated in the ground state, the $d_{5/2}$ orbital is fragmented over several MeV; furthermore, by aligning the low-lying 5^- peak (at $E_x=0.9$ MeV) observed in the ^{40}Ca(p,n)^{40}Sc spectrum with the observed $d_{3/2}$-hole state, one sees that the fragmented 6^- strength aligns well with the observed $d_{5/2}$-hole strength. Considering the comparison shown in Fig. 18, and other evidence for the fragmentation of the $d_{5/2}$-hole state from pickup reactions,[37,38] we would be surprised if the 6^- stretched state were not fragmented also.

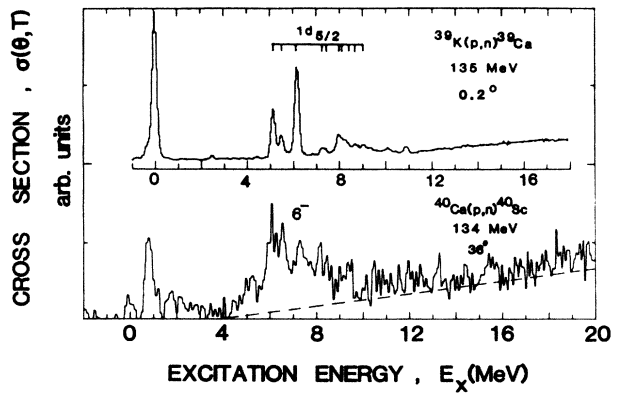

FIG. 18. Comparison of the $d_{5/2}$-hole strength in ^{39}Ca as observed with the ^{39}K(p,n)^{39}Ca reaction at 0.2° to the fragmentation of the 6^- stretched-state strength observed in the ^{40}Ca(p,n)^{40}Sc reaction. The ^{39}K(p,n)^{39}Ca spectrum is from Ref. 37.

It should be noted that the (p,n) reaction, as presented here, provides a superior probe of the $T=1$ strength on a self-conjugate nucleus than does the (p,p') reaction which will excite $T=0$ strength as well. For cases such as the present one, where the isovector strength is fragmented, the suppression of the isoscalar background is critical for identifying the isovector strength unambiguously. For the study of fragmented stretched states, the (p,n) reaction is superior also to backward-angle inelastic electron scattering (which preferentially excites isovector strength) because the electron scattering will not provide the important suppression of the normal parity states as well.

The normalization factor required for the DWIA 6^- calculation is 0.35. It is significant that this factor is greater than that observed for the 6^-, $T=1$ stretched state observed in $A=28$ via (p,p'), (p,n), and (e,e') excitations,[39–41] analyzed in a similar fashion. Presumably, the increased spectroscopic factor observed for $A=40$ is due to a greater filling of the $d_{5/2}$ orbital in ^{40}Ca than in ^{28}Si.

V. DISCUSSION AND CONCLUSIONS

The ^{40}Ca(p,n)^{40}Sc reaction at 134 MeV shows strong excitation of several low-lying states in good agreement with distorted-wave-impulse-approximation calculations with simple 1p1h wave functions[12] for isovector states in ^{40}Sc. This good agreement indicates that these states are predominantly 1p1h in structure and further corroborates the idea that the (p,n) reaction above 100 MeV preferentially excites such strength in even-even nuclei. The agreement observed here between such calculations and experiment is similar to that reported earlier[1] for the (p,n) reaction on ^{16}O.

Several low-lying transitions are observed with structures predicted to be predominantly $(f_{7/2},d_{3/2}^{-1})$ (viz., 2^-, 3^-, 4^-, and 5^- states). These excitations involve the valence levels for ^{40}Ca and apparently the low-lying excitations in ^{40}Sc are dominated by this 1p1h structure. These states are all observed within 1 MeV of the ground state, which is known to be the 4^- state of this band. At slightly higher excitation energy ($E_x=2.3$ MeV), we see a complex of states which is dominated by an $L=3$ angular distribution at wide angles. We interpret this complex to correspond to the excitation of a 4^- state predicted to be at this excitation energy with the predominant structure $(f_{7/2},2s_{1/2}^{-1})$.

In order to try to understand why the DWIA normalization factors are so small for the 2^-–5^- $(f_{7/2},d_{3/2}^{-1})$

band of states, we performed a shell-model calculation which considered only the $d_{3/2}$ and $f_{7/2}$ orbitals, but allowed multiparticle, multihole configurations. The calculation was performed with the shell-model code OXBASH of Brown *et al.*,[31] and the interaction of Sakakura, Arima, and Sebe.[32] This is the same kind of calculation performed to try to describe the observed 1^+ excitations described above. The results of DWIA calculations performed with the wave functions so obtained yield angular distributions similar in shape to the DWIA calculations shown in Figs. 4 and 6, but with significantly increased normalization factors. The normalizations increase as follows: the 2^- goes from 0.18 to 0.25, the 3^- goes from 0.09 to 0.20, the 4^- from 0.09 to 0.20, and the 5^- from 0.20 to 0.30. Note that the smallest normalization factors required with the TDA wave functions increase relatively more, which indicates that such multiparticle, multihole configurations apparently affect these states the most. Clearly, these changes indicate that at least some of the reason for the small normalization factors is the need to consider multiparticle-multihole correlations in the target and configuration mixing in the final nucleus. Presumably, if the basis could be enlarged beyond consideration of just the $d_{3/2}$ and $f_{7/2}$ orbitals, further increases in the extracted normalization factors would be required.

Direct evidence for ground-state correlations in the ^{40}Ca target is provided by the 1^+ excitations observed at $E_x = 2.7$ and 4.3 MeV in this reaction. These positive-parity transitions must proceed primarily from holes in the s-d shell core of ^{40}Ca and/or particles in the $1f$-$2p$ shell. The parent states in ^{40}Ca of these two excitations were observed in the ^{40}Ca(p,p′) reaction, but only the lower one was observed in ^{40}Ca(e,e′) studies, which indicates interference effects between spin and orbital contributions for the higher state. The total strength observed for these two transitions in the (p,n) reaction is each approximately $\frac{1}{15}$ of the strength observed for the low-lying 1^+ excitation in the ^{48}Ca(p,n)^{48}Sc (2.52 MeV) reaction. The latter excitation is believed to be predominantly $(f_{7/2}, f_{7/2}^{-1})$, with nearly the full strength of the eight neutrons in the $f_{7/2}$ shell available. Thus, from this comparison, the 1^+ strength observed in the ^{40}Ca(p,n)^{40}Sc reaction corresponds to approximately one-half of a neutron (hole) available in the $f_{7/2}$ ($d_{3/2}$) orbital. This result is consistent with measured pickup spectroscopic factors; furthermore, the observed 1^+ strength is consistent with DWIA calculations based on wave functions obtained considering core correlations with the simple basis discussed above for consideration of the effects of such correlations on the normalization factors for the low-lying $2^- - 5^-$ band of states.

At higher excitation energies, we see the $L=1$ giant resonance and the 6^- $(f_{7/2}, d_{5/2}^{-1})$ stretched-state strength. Both of these involve particle and/or hole states away from the valence levels and are observed to be fragmented. The $L=1$ strength is observed to be distributed broadly from about 6 to 18 MeV of excitation, and is a dominant feature of the forward-angle spectra. This distribution of $L=1$ strength is in general agreement with the predicted distribution of such strength (i.e., for 0^-, 1^-, and 2^- states) from the TDA shell-model calculations; however, the total strength observed is only about 16% of that calculated in the DWIA with these simple wave functions. The 6^- stretched-state strength is seen to be spread out from about 4 to 10 MeV of excitation and dominates the wide-angle spectra. The fragmentation of this strength is ascribed primarily to the fragmentation of the $d_{5/2}$-hole strength near $A=40$, as observed in the ^{39}K(p,n)^{39}Ca reaction and the ^{40}Ca(p,d)^{39}Ca neutron pickup reaction. The normalization factor required for a DWIA calculation to agree in magnitude with this strength is 0.35. This normalization factor is somewhat larger than that required for a similar analysis of the 6^- stretched-state strength in $A=28$; this result is believed to be due to the fact that the $d_{5/2}$ orbital near $A=40$, while fragmented, is more nearly full than for $A=28$.

In summary, the strongest excitations observed in the ^{40}Ca(p,n)^{40}Sc reaction at 134 MeV generally agree well with DWIA calculations with simple 1p1h (TDA) wave function. High-lying excitations are observed to be fragmented, presumably because of configuration mixing with multiparticle, multihole configurations. Spectroscopic factors of less than 0.5 are obtained from DWIA calculations and are ascribed to the combined effects of ground-state correlations in ^{40}Ca, configuration mixing in the final nucleus, and meson-exchange currents not included in the DWIA. Direct evidence for ground-state correlations is provided by observed 1^+ excitations. The (p,n) reaction is seen to be an excellent probe for 1p1h strength, even when that strength is fragmented.

ACKNOWLEDGMENTS

We are grateful to the staff of the Indiana University Cyclotron Facility for their assistance during the running of this experiment. We thank Peter Tandy, Robert McCarthy, and Alex Brown for helpful discussions concerning the theoretical calculations and interpretation. This work was supported in part by the National Science Foundation under Grants No. PHY 82-00562, No. PHY 85-01054, and No. PHY 81-14339.

[1]A. Fazely, B. D. Anderson, M. Ahmad, A. R. Baldwin, A. M. Kalenda, R. J. McCarthy, J. W. Watson, R. Madey, W. Bertozzi, T. N. Buti, J. M. Finn, M. A. Kovash, B. Pugh, and C. C. Foster, Phys. Rev. C **25**, 1760 (1982).

[2]B. D. Anderson, A. Fazely, R. J. McCarthy, P. C. Tandy, J. W. Watson, R. Madey, W. Bertozzi, T. N. Buti, J. M. Finn, J. Kelly, M. A. Kovash, and B. Pugh, Phys. Rev. C **27**, 1387 (1983).

[3]B. D. Anderson, T. Chittrakarn, A. R. Baldwin, C. Lebo, R. Madey, R. J. McCarthy, J. W. Watson, B. A. Brown, and C. C. Foster, Phys. Rev. C **31**, 1147 (1985).

[4]B. D. Anderson, T. Chittrakarn, A. R. Baldwin, C. Lebo, R.

Madey, R. J. McCarthy, J. W. Watson, B. A. Brown, and C. C. Foster, Phys. Rev. C **31**, 1161 (1985).

[5]B. D. Anderson, C. Lebo, A. R. Baldwin, T. Chittrakarn, R. Madey, and J. W. Watson, C. C. Foster, Phys. Rev. Lett. **52**, 1872 (1984).

[6]J. Kelly and J. A. Carr, in *Spin Excitations in Nuclei,* edited by F. Petrovich *et al.* (Plenum, New York, 1984), p. 253.

[7]A. D. Bacher, in *Polarization Phenomena in Nuclear Physics 1980,* edited by G. G. Ohlsen *et al.* (AIP, New York, 1981), p. 220.

[8]H. O. Meyer, J. R. Hall. W. W. Jacobs, P. Schwandt, and P. P. Singh, Phys. Rev. C **24**, 1782 (1981).

[9]H. O. Meyer, P. Schwandt, W. W. Jacobs, and J. R. Hall, Phys. Rev. C **27**, 459 (1983).

[10]P. J. Brussard and P. W. M. Glaudemans, *Shell-Model Applications in Nuclear Spectroscopy* (North-Holland, Amsterdam, 1977), p. 369.

[11]F. A. Gareev, M. Gmitro, S. N. Ershov, J. Cejpek, Yad. Fiz. **42**, 20 (1985) [Sov. J. Nucl. Phys. **42**, 11 (1985)].

[12]T. W. Donnelly and G. E. Walker, Ann. Phys. (N.Y.) **60**, 209 (1970).

[13]C. D. Goodman, C. C. Foster, M. B. Greenfield, C. A. Goulding, D. A. Lind, and J. Rapaport, IEEE Trans. Nucl. Sci. **NS-26**, 2248 (1979).

[14]R. Madey, J. W. Watson, M. Ahmad, B. D. Anderson, A. R. Baldwin, A. L. Casson, W. Casson, R. A. Cecil, A. Fazely, J. N. Knudson, C. Lebo, W. Pairsuwan, R. J. Pella, J. C. Varga, and T. R. Witten, Nucl. Instrum. Methods **214**, 401 (1983).

[15]A. R. Baldwin and R. Madey, Nucl. Instrum Methods **197**, 379 (1982).

[16]R. Cecil, B. D. Anderson, and R. Madey, Nucl. Instrum. Methods **161**, 439 (1979).

[17]B. D. Anderson, J. N. Knudson, R. Madey, and C. C. Foster, Nucl. Instrum. Methods **169**, 153 (1980).

[18]J. W. Watson, B. D. Anderson, A. R. Baldwin, C. Lebo, B. S. Flanders, W. Pairsuwan, R. Madey, and C. C. Foster, Nucl. Instrum. Methods **215**, 413 (1983); J. D'Auria, M. Dombsky, L. Moritz, T. Ruth, G. Sheffer, T. E. Ward, C. C. Foster, J. W. Watson, B. D. Anderson, and J. Rapaport, Phys. Rev. C **30**, 1999 (1984).

[19]P. M. Endt, and C. van der Leun, Nucl. Phys. **A310**, 1 (1978).

[20]B. D. Anderson, A. R. Baldwin, A. M. Kalenda, R. Madey, J. W. Watson, C. C. Chang, H. D. Holmgren, R. W. Koontz, and J. R. Wu, Phys. Rev. Lett. **46**, 226 (1981).

[21]A. M. Kalend, B. D. Anderson, A. R. Baldwin, R. Madey, J. W. Watson, C. C. Chang, H. D. Holmgren, R. W. Koontz, J. R. Wu, and H. Machner, Phys. Rev. C **28**, 105 (1983).

[22]P. R. Bevington, K. G. Kibler, and B. D. Anderson, Case Western Reserve University Report No. C00-1573-63, 1969 (unpublished); P. R. Bevington, *Data Reduction and Error Analysis for the Physical Sciences* (McGraw-Hill, New York, 1969), p. 237.

[23]*Polarization Phenomena in Nuclear Reaction,* edited by H. H. Barschall and W. Haeberli (University of Wisconsin Press, Madison, 1970).

[24]P. Schwandt, H. O. Meyer, W. W. Jacobs, A. D. Bacher, S. E. Vigdor, M. D. Kaitchuck, T. R. Donoghue, Phys. Rev. C **26**, 55 (1982).

[25]J. Raynal and R. Schaeffer, computer code DWBA 70 (unpublished). The version we used was supplied to us by W. G. Love.

[26]W. G. Love and M. A. Franey, Phys. Rev. C **24**, 1073 (1981).

[27]G. Eulenberg, D. I. Sober, W. Steffen, H. D. Graf, G. Kuchler, A. Richter, E. Spamer, B. C. Metsch, and W. Knupfer, Phys. Lett. **116B**, 113 (1982); K. E. Rehm, P. Kienle, D. W. Miller, R. E. Segel, and J. R. Comfort, *ibid.* **114B**, 15 (1982).

[28]G. M. Crawley, N. Anantaraman, A. Galonsky, C. Djalali, N. Marty, A. Willis, and J. C. Jourdain, Phys. Lett. **127B**, 322 (1983).

[29]T. N. Taddeucci, J. Rapaport, C. C. Foster, C. D. Goodman, C. Gaarde, J. Larsen, C. A. Goulding, D. J. Horen, T. Masterson, and E. Sugarbaker, Phys. Rev. C **28**, 2511 (1983).

[30]P. M. Endt, At. Data Nucl. Data Tables **19**, 23 (1977).

[31]B. A. Brown, A. Etchezoyen, W. D. M. Ral, and N. S. Godwin, private communication from B. A. Brown.

[32]M. Sakakura, A. Arima, and T. Sebe, Phys. Lett. **61B**, 335 (1976).

[33]B. D. Anderson, R. J. McCarthy, M. Ahmad, A. Fazely, A. M. Kalenda, J. N. Knudson, J. W. Watson, R. Madey, and C. C. Foster, Phys. Rev. C **26**, 8 (1982).

[34]B. D. Anderson, J. W. Watson, C. Lebo, A. R. Baldwin, A. Fazely, R. Madey, and C. C. Foster, Phys. Lett. **123B**, 383 (1983).

[35]F. Petrovich and W. G. Love, Nucl. Phys. **A354**, 499c (1981).

[36]J. W. Watson, W. Pairsuwan, B. D. Anderson, A. R. Baldwin, B. S. Flanders, R. Madey, R. J. McCarthy, B. A. Brown, B. H. Wildenthal, and C. C. Foster, Phys. Rev. Lett. **55**, 1369 (1985).

[37]J. Källne and B. Fagerström, Phys. Scr. **11**, 79 (1975).

[38]J. W. Watson, M. Ahmad, D. W. Devins, B. S. Flanders, D. L. Friesel, N. S. Chant, P. G. Roos, and J. Wastell, Phys. Rev. C **26**, 961 (1982).

[39]C. Olmer, A. D. Bacher, G. T. Emery, W. P. Jones, D. W. Miller, H. Nann, and P. Schwandt, S. Yen, T. E. Drake, and R. J. Sobie, Phys. Rev. C **29**, 361 (1984).

[40]A. Fazely, R. Madey, B. D. Anderson, A. R. Baldwin, C. Lebo, J. W. Watson, W. Bertozzi, T. Buti, M. Finn, C. Hyde, J. Kelly, B. Pugh, and C. C. Foster, Bull. Am. Phys. Soc. **27**, 629 (1982).

[41]R. Lindgren and F. Petrovich, in *Spin Excitations in Nuclei,* edited by F. Petrovich *et al.* (Plenum, New York, 1984), p. 323.